Beyond One-Electron Reaction in Li Cathode Materials: Designing $Li_2Mn_xFe_{1-x}SiO_4$

Anton Kokalj,[†] Robert Dominko,[‡] Gregor Mali,[‡] Anton Meden,[§] Miran Gaberscek,*[,‡] and Janez Jamnik[‡]

Jozef Stefan Institute, Jamova 39, SI-1000 Ljubljana, Slovenia, National Institute of Chemistry, Hajdrihova 19, SI-1000 Ljubljana, Slovenia, Faculty of Chemistry and Chemical Technology, Askerceva 5, SI-1000 Ljubljana, Slovenia.

Received December 19, 2006. Revised Manuscript Received April 5, 2007

Li_2MnSiO_4 has been identified recently as one of the first cathode battery materials that, at least in principle, could exchange more than 1 lithium per redox-active transition metal ion. In this article, we analyze experimentally and by computer simulations based on density functional theory (DFT) why actual experiments have not confirmed these expectations. We show that Li_2MnSiO_4 is unstable upon delithiation, with a strong tendency to amorphize. Detailed DFT calculations further indicate that it might be possible to obtain a stable material with a reversible exchange of more than one Li per formula unit (FU) by using an appropriate Mn/Fe mixture (solid solution) with a general formula $Li_2Mn_xFe_{1-x}SiO_4$.

1. Introduction

Although many classes of materials for positive electrodes in lithium batteries have been thoroughly investigated in the past two decades, no real gain in capacity has been achieved.[1] Recently, two materials from a new family of transition metal silicates, namely Li_2FeSiO_4 and Li_2MnSiO_4, have been successfully prepared and preliminary tested as potential positive electrode materials (cathodes) for lithium-ion batteries.[2,3] Although the primary motivation for preparation of these materials was their low price and safety (the thermal stability of Li_2MnSiO_4 is shown in the Supporting information, Figure S1), it was hoped that at least the Li_2MnSiO_4 analogue could open exciting new prospects in the search for high-capacity cathode materials. Namely, unlike iron, which in compounds primarily appears in the formal oxidation states of Fe^{II} and Fe^{III}, manganese is regularly found in higher oxidation states. Simply stated, if more than 1 Li per formula unit (FU) were extracted from Li_2MnSiO_4, Mn^{III} (which formally appears in $LiMnSiO_4$) could be further oxidized to Mn^{IV}, leading to a fully delithiated $Mn^{IV}SiO_4$ compound. Provided that the structure of this compound was stable, a reversible exchange of up to two lithium ions per FU (and a capacity above 300 mA h g^{-1}) would become possible. This would certainly represent one of the most important breakthroughs in the field of cathode materials since the invention of Li-ion batteries in 1991. Our first testings of Li_2MnSiO_4, however, did not hold that promise,[2] showing a reversible capacity of only about 100 mA h g^{-1}. Although much higher values have also been obtained in further testing (up to 270 mA h g^{-1}), this only occurred sporadically. In this paper, we clearly demonstrate, experimentally and using DFT calculations, that the delithiated structure of parent Li_2MnSiO_4 is inherently unstable and tends to collapse. Atomistic simulations further show that mixing with Li_2FeSiO_4 could yield the optimal compromise between structural stability and high utilization of lithium.

2. Technical Details

2.1. Experimental Section. Li_2MnSiO_4 was prepared by dispersing 6 nm SiO_2 particles in water and stabilizing them with citric acid and ethylene glycol. We used acetate and nitrate precursors for cations. Li_2MnSiO_4 was prepared at temperatures higher than 700 °C in an Ar atmosphere. Depending on the cation precursor used, the amount of carbon in as-synthesized samples was between 0 and 4 wt %. The yield of Li_2MnSiO_4 with this type of synthesis is at least 95%. MnO_2 was found to be the main impurity. Particle size was between 30 and 500 nm, depending on temperature and on the type of precursors used. Electrochemical measurements: 10 wt % CB + 10 wt % PVdF dispersed in NMP + 80 wt % as-prepared material, ball milled for 1 h, dispersed onto Al foil, and dried at 120 °C overnight. Electrodes had a geometric area of 2 cm^2. A two-electrode cell (coffee bag) with metallic lithium as a reference and a counter electrode was used. Current density: *C*/20. Cutoff voltage: 4.2 and 2.0 V. In situ XRD measurements were taken on samples in which Li was gradually extracted at a constant rate of *C*/50. ^{6}Li magic-angle spinning (MAS) NMR spectra were recorded on a Varian Unity Inova 600 spectrometer, operating at ^{6}Li Larmor frequency of 88.274 MHz, with a rotation-synchronized Hahn-echo pulse sequence. The sample rotation frequency was 22.73 kHz, the repetition delay between consecutive scans was 1 s, and the number of scans was between 20 000 and 100 000. In all spectra, the frequency axis in parts per million is reported relative to the signal of lithium nuclei within a 1 M solution of LiCl. All NMR samples were carefully weighed before measurements. Because all other parameters of the measurements were kept fixed, the integrated intensities of the recorded spectra enabled us to roughly compare the amount of Li within different samples.

* Corresponding author. E-mail: miran.gaberscek@ki.si.
† Jozef Stefan Institute.
‡ National Institute of Chemistry.
§ Faculty of Chemistry and Chemical Technology.

(1) Tarascon, J. M.; Armand, M. *Nature* **2001**, *414*, 359.
(2) Dominko, R.; Bele, M.; Gaberscek, M.; Meden, A.; Remskar, M.; Jamnik, J. *Electrochem. Commun.* **2006**, *8*, 217.
(3) Nyten, A.; Abouimrane, A.; Armand, M.; Gustaffson, T.; Thomas, J. O. *Electrochem. Commun.* **2005**, *7*, 156.

10.1021/cm063011l CCC: $37.00
Published on Web 06/29/2007

2.2. Computational Methods. The calculations were performed in the framework of density functional theory, using the generalized gradient approximation of Perdew−Burke−Ernzerhof.[4] We used the pseudopotential method with ultra-soft pseudopotentials.[5,6] Kohn−Sham orbitals were expanded in a plane-wave basis set up to a kinetic energy cutoff of 50 Ry (400 Ry for the charge-density cutoff). Structures were optimized using damped variable cell shape Wentzcovitch molecular dynamics.[7] After optimization, all structures were recalculated so as to account for the change in basis set. The Brillouin zone corresponding to the (1 × 1 × 1) unit cell was sampled by 4 × 4 × 4 uniformly shifted k-mesh,[8,9] whereas for a (1 × 2 × 1) supercell, a 4 × 2 × 4 k-mesh was used. The calculations were performed spin-polarized with the ferromagnetic (FM) configuration, although the anti-FM solutions have lower energies for a few tested cases. The differences, however, are small, on the order of 10 meV/FU. All calculations have been done using the PWscf code contained in the Quantum ESPRESSO distribution,[10] whereas molecular graphics were produced by the XCRYSDEN graphical package.[11]

3. Results and Discussion

3.1. Experimental Analysis of Li_2MnSiO_4. Although the theoretical capacity of Li_2MnSiO_4 is about 333 mA h g^{-1},[2,12] a large number of experiments performed in our laboratory have given an average capacity value of only about 100 mA h g^{-1}, even at very low charge−discharge currents of C/50 (about 6.6 mA per gram of active material). These low practical capacities were initially attributed to the extremely low conductivity of Li_2MnSiO_4 (Figure 1a), that is, by about 2 orders of magnitude lower than for Li_2FeSiO_4 at a given temperature. In an effort to minimize this problem, we have used two standard approaches, such as particle-size reduction and carbon-decoration techniques that proved very efficient in the case of another poorly conducting material, $LiFePO_4$.[13−15] Contrary to expectations, such materials engineering has not led to a significant improvement of the performance of Li_2MnSiO_4. In the course of these extensive experiments, however, we[16] and other authors[17] have sporadically observed unusually high reversible capacities (up to 285 mA h g^{-1}, corresponding to the exchange of up to 1.75 Li/FU). These high reversible capacities have only been observed in the initial cycles, and they then rapidly decreased to the typical values of about 100 mA h g^{-1} (Figure 1b). Importantly, the rare charge−discharge curves that have delivered the high capacities have always exhibited a different shape (shape A

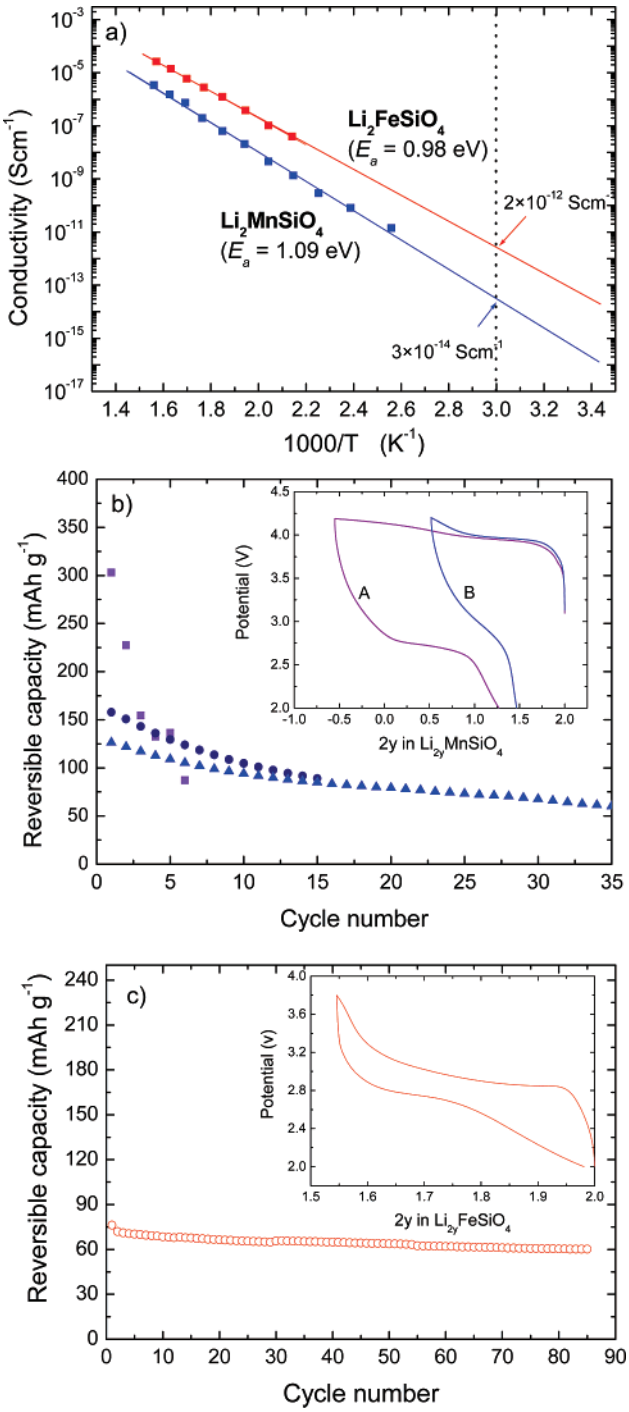

Figure 1. Electrical and electrochemical characterization of Li_2FeSiO_4 and Li_2MnSiO_4. (a) Temperature dependence of conductivity. The values at 60 °C and the activation energies are explicity shown. (b) Reversible capacity of Li_2MnSiO_4 as a function of cycle number. Note the two types of degradation (type A, squares; type B, circles and triangles). Inset: Two characteristic shapes of charge−discharge curve observed for Li_2MnSiO_4: (A) shape typical for high capacities (>200 mA h g^{-1}), (B) shape typical for low capacities (<130 mA h g^{-1}). (c) Reversible capacity of Li_2FeSiO_4 as a function of cycle number. Inset: The shape of charge−discharge curve for Li_2FeSiO_4. The notation for variable average Li content (2*y*) is used so as to be compatible with eq 2 (see the theoretical part).

(4) Perdew, J. P.; Burke, K.; Ernzerhof, M. *Phys. Rev. Lett.* **1999**, *77*, 3865.
(5) Vanderbilt, D. *Phys. Rev. B* **1990**, *41*, 7892.
(6) Ultrasoft pseudopotentials for Li, Mn, Fe, Si, and O were taken from the *PWscf PseudoPotential Download Page*: http://www.pwscf.org/pseudo.htm (files: Li.pbe-s-van_ak.UPF, Mn.pbe-sp-van.UPF, Fe.pbe-sp-van.UPF, Si.pbe-rrkj.UPF, and O.pbe-rrkjus.UPF).
(7) Wentzcovitch, R. *Phys. Rev. B* **1991**, *44*, 2358.
(8) Monkhorst, H. J.; Pack, J. D. *Phys. Rev. B* **1976**, *13*, 5188.
(9) Bonini, N.; Kokalj, A.; Dal Corso, A.; de Gironcoli, S.; Baroni, S. *Phys. Rev. B* **2004**, *69*, 195401.
(10) Baroni, S.; et al. http://www.quantum-espresso.org/ (2005).
(11) Kokalj, A. *Comput. Mater. Sci.* **2003**, *28*, 155. Code available from http://www.xcrysden.org/.
(12) Arroyo-de Dompablo, M. E.; Armand, M.; Tarascon, J. M.; Amador, U. *Electrochem. Commun.* **2006**, **8**, 1292.
(13) Armand, M.; Gauthier, M.; Magnan, J. F.; Ravet, N. World Patent WO 02/27823 A1, 2002.
(14) Dominko, R.; Bele, M.; Gaberscek, M.; Remskar, M.; Hanzel, D.; Pejovnik, S.; Jamnik, J. *J. Electrochem. Soc.* **2005**, *152*, A607.
(15) Moskon, J.; Dominko, R.; Gaberscek, M.; Cerc-Korosec, R.; Jamnik, J. *J. Electrochem. Soc.* **2006**, *153*, A1805.
(16) Dominko, R.; et al. Presented at the International Meeting on Lithium Batteries (IMLB 2006), Biarritz, France; Electrochemical Society: Pennington, NJ, 2006; Abstract 214.
(17) Li, Y.; Gong, Z.; Yang, Y. Presented at the International Meeting on Lithium Batteries (IMLB 2006), Biarritz, France; Electrochemical Society: Pennington, NJ, 2006; Abstract 210.

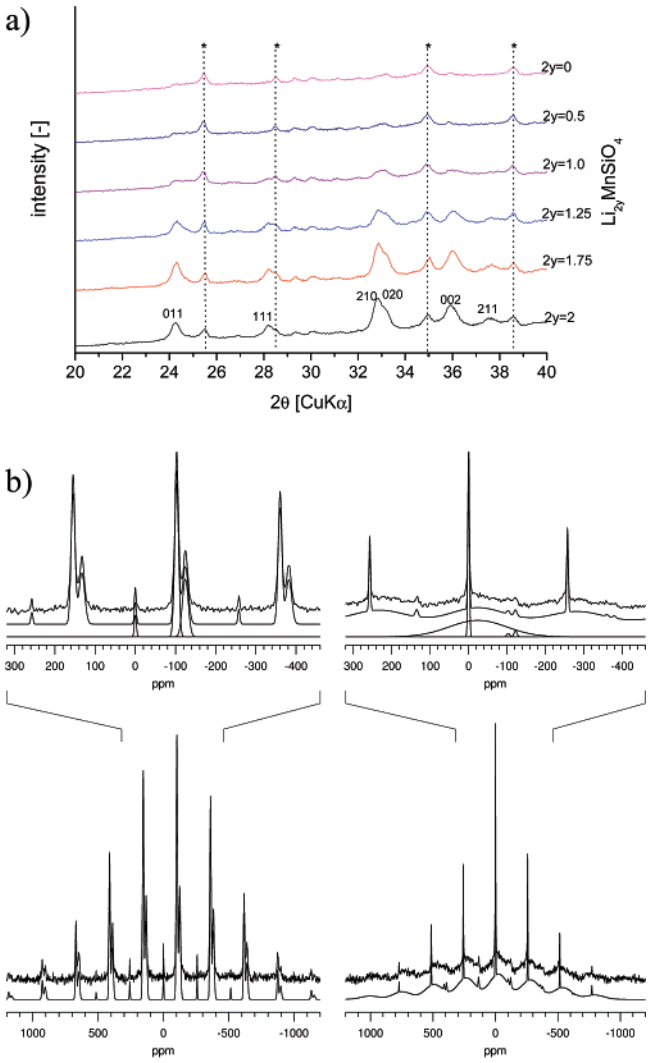

Figure 2. (a) In situ X-ray diffraction measurements of $Li_{2y}MnSiO_4$ as a function of *y* (note: the notation, 2*y*, is adjusted to corrrespond to that used in eq 2). Asterisk (*) denotes the peaks originating from the measurement cell, the lower diffractogram with Miller indices corresponds to the *Pmn*2_1 structure for Li_2MnSiO_4. (b) ^{6}Li MAS NMR spectra of the parent Li_2MnSiO_4 (left) and of the material obtained after one completed charge−discharge cycle (right). The measured spectra including the broad patterns of spinning sidebands were decomposed into several contributions. Isotropic bands are shown in the top insets.

in the inset of Figure 1b), if compared to the typical low-capacity charge−discharge curves (shape B in the inset of Figure 1b). By contrast, for Li_2FeSiO_4, only one type of charge−discharge curve was observed (Figure 1c, inset), yielding a relatively stable capacity of 70 mA h g^{-1} (Figure 1c) or even higher.[3]

On the basis of these results, we have assumed that, upon delithiation, the original Li_2MnSiO_4 structure becomes unstable and tends to transform, more or less rapidly, into other structure(s). Using in situ X-ray diffractometry, however, rather than new structure(s), a progressive loss of the initial peaks can be observed during delithiation (Figure 2a). In consecutive cycling, the initial peaks are not recovered. This result can be interpreted in two ways: either the X-ray peaks fade out simply because of a substantial decrease in the average size of crystallites, or the initial structure is progressively amorphized during delithiation. The results of solid-state NMR (Figure 2b), which show significant changes in the ^{6}Li MAS spectrum after completion of the first charge−discharge cycle, seem to support the latter scenario. The two most intense sets of sharp signals in the spectrum of the parent Li_2MnSiO_4 vanish almost completely, and a weaker set of much broader signals appears in the spectrum of the cycled material. Probably, the crystalline Li_2MnSiO_4 collapses during Li extraction, leaving behind an amorphous-like phase.

Assignment of different NMR signals is difficult. As shown in our previous paper,[2] a substantial structural disorder can be found in Li_2MnSiO_4 materials. In addition to the main Li and Mn sites, there also exist alternative Li and Mn sites in the structure. Furthermore, part of the Li ions within the material can occupy Mn sites and vice versa. All these effects are responsible for several different environments around the Li nuclei and can therefore lead to the appearance of several peaks in ^{6}Li MAS NMR spectra (see the Supporting Information, Figures S2−S4). Isotropic shifts of resonance lines of Li spectra are primarily determined by the hyperfine coupling (or transferred hyperfine coupling) between Li nuclei and unpaired electrons of Mn atoms. Because the magnitude of the coupling depends on the number of Mn atoms in the second coordination shell around a Li ion, a negligible isotropic shift of Li NMR signal at about 0 ppm suggests that the corresponding Li nuclei do not exhibit Li−O−Mn bonds. On the other hand, their pattern of spinning sidebands is as broad as the patterns of other Li NMR signals, indicating that they still feel relatively strong "through-space" dipolar interaction with paramagnetic centers. The signal can therefore be attributed to Li ions that either belong to a paramagnetic Li−Mn impurity or occupy Mn sites within Li_2MnSiO_4. The other NMR signals exhibit larger isotropic shifts, showing that they occupy slightly different Li sites within Li_2MnSiO_4.

A rough quantitative comparison of the two spectra shown in Figure 2b reveals that the composition of the cycled material is approximately $Li_{0.8}MnSiO_4$. In addition to line-broadening, Li extraction and reinsertion also induces a shift of the NMR signals; isotropic shifts of −103 and −125 ppm are found for the two sharp contributions in the spectrum of the parent material, and an isotropic shift of −24 ppm is found for the broad contribution in the spectrum of the cycled material. The observed shift of the lithium NMR signal suggests that in the cycled material, hyperfine coupling between lithium nuclei and unpaired electrons from manganese is smaller than in the parent Li_2MnSiO_4. Such a reduction of the coupling could be induced by a change of Mn oxidation state, by a decreased number of Mn atoms in the second coordination shell around Li, or by formation of Li−O−Mn bonds with a weaker covalent character.

The experimental results indicate coherently that, unlike in the case of Li_2FeSiO_4,[3] the original structure of Li_2MnSiO_4 is unstable upon delithiation, with a strong tendency to amorphize. Further important information about the structural changes upon delithiation of Li_2MnSiO_4 has been obtained by TEM examination of partly delithiated samples (Figure 3). After nominal extraction of about 50% of Li, that is, in a sample with average composition of $LiMnSiO_4$, the original structure (Figure 3a) is obviously coexistent with amorphous-like regions (Figure 3b). This result strongly suggests that

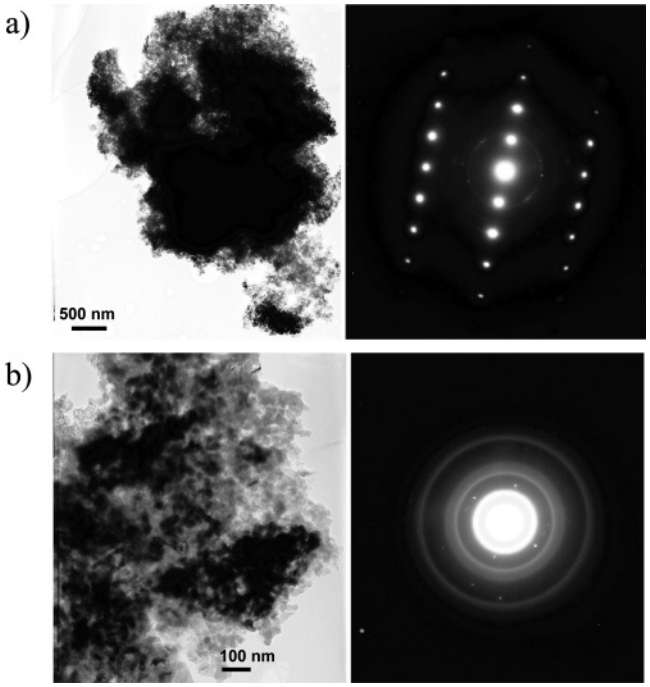

Figure 3. TEM and electron diffraction pattern of partly charged $Li_{2y}MnSiO_4$ (y = ca. 1/2). The upper (a) and lower (b) results were obtained by examining different locations of the same active material. Detailed investigation of several tens of surface spots always revealed these two typical patterns.

delithiation does not proceed uniformly but most likely via a phase-separation mechanism such as, for example, that found in olivines.[18,19]

3.2. Density Functional Theory Calculations: Design of an Improved Material. Evolution of structural and electronic properties of Li_2MnSiO_4 during delithiation can be further investigated by DFT calculations. Indeed, in their recent study, Larsson et al.[20] applied such calculations to electrochemically characterize Li_2FeSiO_4, whereas Arroyo-de Dompablo et al.[12] correlated the calculated open circuit voltage of Li_2MXO_4 family of compounds (M = Fe, Mn, Co, Ni; X = Ge, Si, Sb, As, P) to Mulliken electronegativity of X. In the present work, we try to explain the reasons for the structural collapse of Li_2MnSiO_4 during delithiation and, in particular, find ways for stabilization of this structure while preserving the inherent high capacity of Li_2MnSiO_4-based materials. In pursuing this goal, we performed DFT simulations, within the generalized gradient approximation[4] (GGA), on Li_2MnSiO_4, Li_2FeSiO_4, and their mixtures. In all cases, the crystal structure (Figure 4) can be described by an orthorhombic unit cell. For pure compounds Li_2MnSiO_4 and Li_2FeSiO_4, the space group is $Pmn21$.[2]

Experimental and calculated lattice parameters are shown in Table 1. All ions in Li_2MSiO_4, M = Mn or Fe, are tetrahedrally coordinated: the cations, M, Li, and Si, are linked to four oxygen atoms, whereas each oxygen atom has one Si, M, and two Li neighbors (see Figure 4).

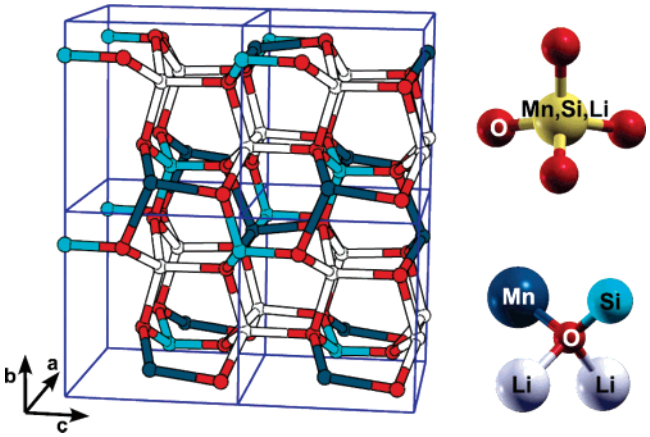

Figure 4. Snapshot of the crystal structure of Li_2MSiO_4, M = Mn, Fe. The two tetrahedra displayed on the right show the local environment of constituent ions: the cations, M (blue balls), Li (white), and Si (cyan), are linked to four oxygen atoms (red), whereas each oxygen atom has one Si, M, and two Li neighbors.

Table 1. Calculated and Experimental Lattice Parameters (a, b, c) and Unit-Cell Volumes (V) for Li_2MSiO_4, M = Mn, Fe, and $Mn_{0.5}Fe_{0.5}$

	a (Å)	b (Å)	c (Å)	V (Å^3)
		Mn		
GGA (this work)	6.30	5.38	5.01	169.5
GGA+U[12]	6.37	5.43	5.04	174.2
expt[2]	6.31	5.38	4.97	168.6
		Fe		
GGA (this work)	6.29	5.35	4.99	167.9
GGA[20]	6.31	5.39	4.98	169.5
GGA+U[12]	6.32	5.58	5.00	170.1
expt[2]	6.27	5.34	4.69	166.1
expt[3]	6.27	5.33	5.02	167.5
expt[21]	6.30	5.53	5.02	174.8
		$Mn_{0.5}Fe_{0.5}$		
GGA (this work)	6.29	5.36	5.00	168.6

There are two Li_2MSiO_4 formula units per unit cell, which means four Li ions/unit cell, and all of them are symmetry-equivalent in pure compounds. When lithium ions are removed from the structure, various lithium-vacancy arrangements can be formed. We consider such arrangements restricted to the (1 × 1 × 1) unit cell.[22] Hence, there can be five different concentrations with 4, 3, 2, 1, and 0 Li ions/unit cell. Normalized to the formula unit of $Li_{2y}MSiO_4$, this corresponds to y = 1, 3/4, 1/2, 1/4, and 0. Note that for Mn/Fe mixtures, the number of possible Li vacancies arrangements does not depend solely on the Li concentration, but also on Mn/Fe composition. We have calculated all possible Li-vacancy arrangements confined to the (1 × 1 × 1) unit cell. In the following, we will consider only the most energetically stable arrangements for $Li_{2y}Mn_xFe_{1-x}SiO_4$, $x \in [0,1]$ and $y \in [0,1]$.

As we progressively remove Li ions from the structure, we monitor the relaxation of the lattice and compare the

(18) Delacourt, C.; Poizot, P.; Tarascon, J. M.; Masquelier, C. *Nat. Mater.* **2005**, *4*, 254.
(19) Yamada, A.; Koizumi, H.; Nishimura, S. I.; Sonoyama, N.; Kanno, R.; Yonemura, M.; Nakamura, T.; Kobayashi, Y. *Nat. Mater.* **2006**, *5*, 357.
(20) Larsson, P.; Ahuja, R.; Nyten, A.; Thomas, J. O. *Electrochem. Commun.* **2006**, *8*, 797.
(21) Quoirin, G.; Dupont, L.; Taulelle, L.; Masquellier, C. Presented at the International Meeting on Lithium Batteries (IMLB 2006), Biarritz, France; Electrochemical Society: Pennington, NJ, 2006; Abstract 211.

(22) We have also considered lithium vacancy arrangements confined to (1 × 2 × 1) supercell and performed corresponding calculations. Indeed, we were able to identify a few slightly more stable (1 × 2 × 1) superstructures compared to the (1 × 1 × 1) cell, but these do not alter any conclusions obtained on the basis of (1 × 1 × 1) unit-cell calculations presented in this work.

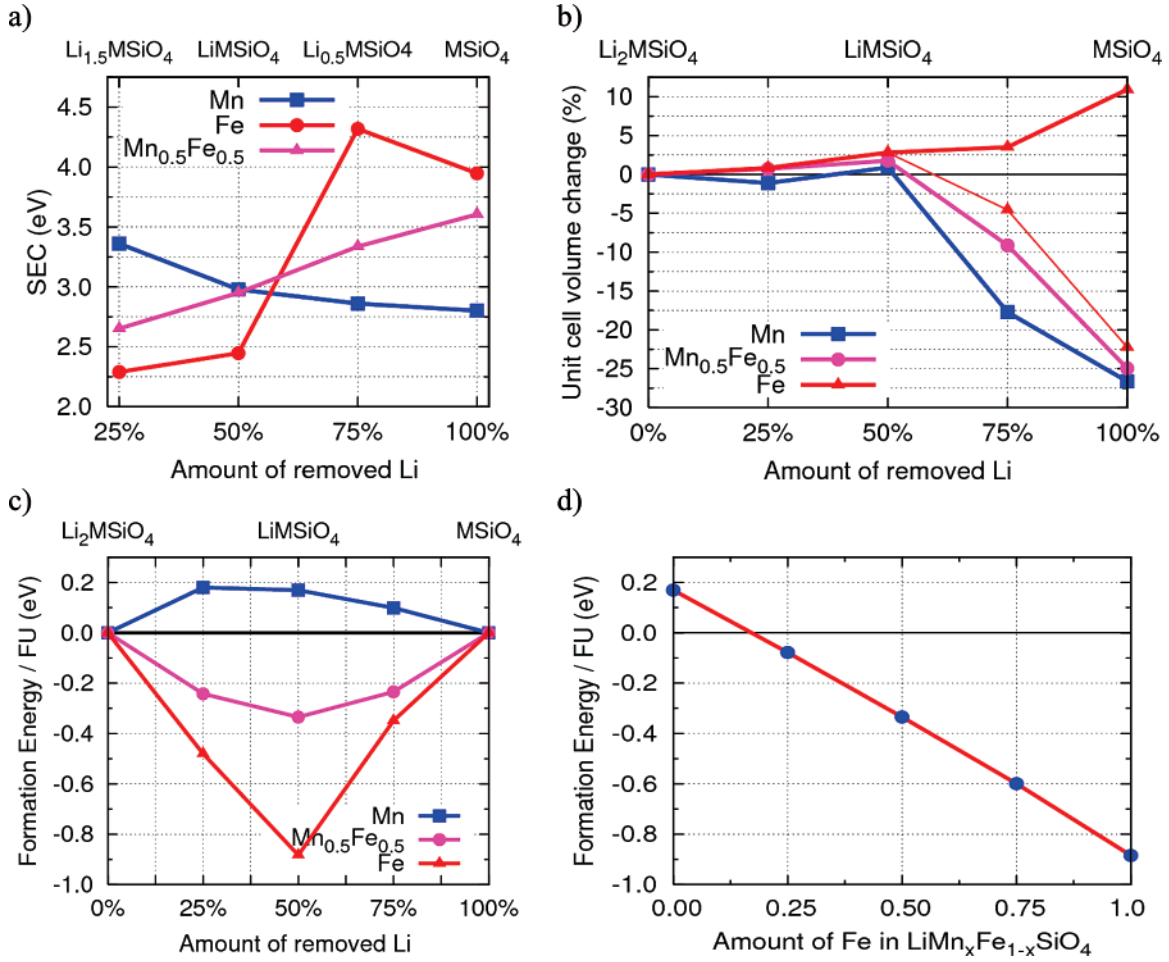

Figure 5. (a) Sequential energy cost (SEC) as defined by eq 1 for the extraction of Li ions from the Li_2MSiO_4, M = Mn (blue line), $Mn_{0.5}Fe_{0.5}$ (violet line), and Fe (red line). The corresponding relative changes of the unit-cell volume are shown in (b). For the explanation of the red thin line, see text. (c) Formation energy ($\Delta\epsilon(y)$, eq 2) of $Li_{2y}MSiO_4$ as a function of y, M = Mn (blue), $Mn_{0.5}Fe_{0.5}$ (violet), and Fe (red). (d) Formation energy of 50% delithiated $LiMn_xFe_{1-x}SiO_4$ as a function of Fe concentration.

relative stabilities of the corresponding structures. As a measure of the relative stabilities, we introduce a sequential energy cost (SEC) for Li extraction

$$\mathrm{SEC}(n) = E(n) - E(n+1) + E_0 \qquad (1)$$

where $E(n)$ is the total energy of the structure with n Li ions in the unit cell, and E_0 is a suitable energy reference; we choose E_0 as the energy of the bulk bcc Li. Note that n is normalized to the unit cell, whereas y appearing in $Li_{2y}MSiO_4$ refers to the formula unit; therefore, the relation between the two is $y = n/4$. As there are only four Li ions in the unit cell, the possible n in SEC(n) ranges from 3 to 0. Thus, for example, SEC(3) measures the energy cost required to remove the first Li ion from the unit cell with respect to bulk bcc lithium. In terms of open circuit voltage (OCV), SEC divided by the unit charge corresponds to the average[23] OCV of the reaction $Li_{(n/2)}MSiO_4 + 1/2Li = Li_{(n+1)/2}MSiO_4$, assuming both compositions are homogeneous (solid solutions). It is known that GGA predicts too small open circuit voltages; underestimations as large as 1 V are not uncommon.[24] We find a similar trend. For example, our calculated average OCV for the reaction $LiMSiO_4 + Li \rightarrow Li_2MSiO_4$ are 3.2 and 2.4 V for M = Mn and Fe, respectively, whereas the experimental values are 4.2 and 3.1 V, respectively.[2] It has been shown[25] recently that an improved estimation of the average OCV can be achieved using the GGA+U method, which yields values of 4.3 and 3.2 V for M = Mn and Fe, respectively.[12]

In panels a and b of Figure 5, we display the SEC values for Li extraction and the corresponding unit-cell volume change (ΔV), respectively. The monotonically decreasing SEC curve for the Mn compound predicts that, in this case, it is the most difficult to remove the first Li ion from the unit cell, whereas to remove the last Li ion is the easiest (thermodynamically). This may suggest that Li_2MnSiO_4 would phase-separate into Li_2MnSiO_4 and $MnSiO_4$ during Li extraction. This issue will be further discussed below in terms of formation energies. On the other hand, the SEC curve for the Fe compound shows that the cost for the removal of the first 50% of Li ions from the unit cell (i.e., passing from Li_2FeSiO_4 to $LiFeSiO_4$) is substantially smaller than for the Mn compound. The cost to extract further Li ions is remarkably higher, > 1.5 eV. This is in good agreement with the results by Arroyo-de Dompablo[12] and

(23) Aydinol, M. K.; Kohan, A. F.; Ceder, G.; Cho, K.; Joannopoulos, J. *Phys. Rev. B* **1997**, *56*, 1354.
(24) Zhou, F.; Cococcioni, M.; Kang, K.; Ceder, G. *Electrochem. Commun.* **2004**, *6*, 1144.
(25) Zhou, F.; Cococcioni, M.; Marianetti, C. A.; Morgan, D.; Ceder, G. *Phys. Rev. B* **2004**, *70*, 235121.

consistent with the experimental results that show that the maximum capacity of Li_2FeSiO_4 is limited to ~1 Li ion/FU[3] when the cut off voltage is limited to moderate potentials slightly above 4 V vs Li reference.

The SEC curve for the mixed $Li_2Mn_{0.5}Fe_{0.5}SiO_4$ system lies between those for the pure compounds. The remarkable difference between the SEC behavior for Mn and Fe compounds is mainly due to the different electronic configuration of the Mn and Fe ions[12] (see the Supporting Information, text S1). In view of this difference in electronic structure, one would, in fact, expect a much larger difference in measured electronic conductivity than that displayed in Figure 1a. We attribute this discrepancy mainly to the fact that real materials always contain a significant amount of impurities, which can drastically alter the conduction mechanism. Other explanations for such deviations have been proposed, especially for olivine phospates, another class of poor intrinsic electron conductors.[26,27]

The Mn and Fe compounds behave rather differently upon delithiation also with respect to volume change, as shown in Figure 5b. The volume of the Fe compound (red line) increases only up to ~3% when passing from Li_2FeSiO_4 to $Li_{0.5}FeSiO_4$, whereas for fully delithiated $FeSiO_4$, the volume is by 11% larger; note that in the latter case, the $FeSiO_4$ layers extending along the (010) plane are completely disconnected from each other because of the absence of Li cations. The electrostatic repulsion between the facing oxygen anions pushes the layers apart. As for the Mn compound (blue line), our calculations reveal a remarkably different behavior. The volume change up to $LiMnSiO_4$ is not much affected, as ΔV remains within 2%. However, upon further delithiation, a very substantial decrease in volume is predicted: a ΔV of -17 and -27% for $Li_{0.5}MnSiO_4$ and $MnSiO_4$, respectively. This is a clear indication of a structural collapse, in full agreement with the experiments shown above.

Once the collapsed structures have been identified, it is possible to check whether similar local minima also exist for the other delithiated compounds. As for the $Li_{0.5}FeSiO_4$ and $FeSiO_4$ compounds, the collapsed structures are energetically similar to the noncollapsed. The unit-cell volume of the collapsed Fe structures is shown by the red thin line in Figure 5b. On the other hand, the collapsed $Li_{0.5}Mn_{0.5}Fe_{0.5}SiO_4$ and $Mn_{0.5}Fe_{0.5}SiO_4$ structures are predicted to be more stable than the noncollapsed by 0.14 and 0.35 eV/FU, respectively. The corresponding unit-cell volumes of $Mn_{0.5}Fe_{0.5}$ compounds are shown in Figure 5b by the purple line. We have also identified a noncollapsed $MnSiO_4$ structure, but it is substantially less stable than the collapsed one (0.70 eV/FU), whereas for $Li_{0.5}MnSiO_4$, only the collapsed structure was found.

The collapsed and noncollapsed delithiated $Li_{0.5}MSiO_4$ and $MSiO_4$ (M = Mn, Fe) structures are significantly different (see Figure 6). In the collapsed structure of fully delithiated $MnSiO_4$, we have observed a peculiar feature: a 5-fold coordinated silicon (see inset in Figure 6). Five-fold coordinated silicon has been reported to be among the abundant defects in amorphous materials.[28] This might be a hint that the structure might become amorphous in reality (our simulated structure is periodic by construction because of use of periodic boundary conditions).

We also calculate formation energies per FU, $\Delta\epsilon(y)$, of $Li_{2y}MSiO_4$ as

$$\Delta\epsilon(y) = \epsilon(y) - [y\epsilon(y=1) + (1-y)\epsilon(y=0)] \qquad (2)$$

where $\epsilon(y)$ is the total energy per FU of the structure with $2y$ Li ions per FU, whereas $\epsilon(y=1)$ and $\epsilon(y=0)$ are the total energies per FU of the Li_2MSiO_4 and fully delithiated $MSiO_4$, respectively. Note the use of symbols E and ϵ in eqs 1 and 2: the first is normalized to the unit cell, whereas the latter is normalized to the formula unit. A negative formation energy means that a compound with given Li concentration is energetically stable. For phase separation to occur at a given temperature, all intermediate structures should have positive formation energies that are large enough to overcome the entropy contribution.

Figure 5c shows formation energies for pure $Li_{2y}MnSiO_4$ and $Li_{2y}FeSiO_4$ compounds and a $Li_{2y}Mn_{0.5}Fe_{0.5}SiO_4$ mixture as a function of Li concentration y. For the whole concentration range y, the formation energies of $Li_{2y}MnSiO_4$ are positive, whereas those for the other two compounds are negative. This indicates that the Mn compound would tend to phase-separate into Li_2MnSiO_4 and $MnSiO_4$ during delithiation, in full accordance with the TEM observation in Figure 3. On the contrary, $Li_{2y}FeSiO_4$ and $Li_{2y}Mn_{0.5}Fe_{0.5}SiO_4$ are not expected to phase separate. Therefore, addition of Fe into the Mn based compound could be one of the strategies leading to stabilization of compositions with intermediate concentrations of Li. From Figure 5d, it is possible to estimate the amount of Fe needed to suppress the phase separation. This figure, which displays the formation energies of 50% delithiated $LiMn_xFe_{1-x}SiO_4$ as a function of the Fe concentration, reveals that at an Fe concentration of around 15% the formation energies become negative.

The phase-separation issues shown above, however, are valid at zero T and P, whereas at finite T and P, the energy ϵ in eq 2 should be replaced by the Gibbs free energy, $G = E + PV - TS$. At $P = 1$ bar, the PV term is on the order of 1×10^{-4} eV/FU and can be neglected, hence $G \approx F = E - TS$, where F is the Helmholtz free energy. The formation free energy is therefore $\Delta g_T(y) \cong \Delta\epsilon(y) - T\{S_T(y) - [yS_T(y=1) + (1-y)S_T(y=0)]\}$. We use the lowercase "$g$" to indicate the formation free energy per FU, whereas subscript "$_T$" indicates the quantity at given T. We have estimated the TS_T term from the experimental measurements of specific heats, C_P (see the Supporting Information, text S2 and Figure S6). At room temperature, the TS_T terms for Li_2MnSiO_4 and Li_2FeSiO_4 have similar values, on the order of 1/4 eV/FU. Note, however, that it is the difference of TS_T terms between various compounds that enters into the formation free energy equation. This difference is likely to be just a fraction of a given TS_T value. For the conclusions stated in the paragraph above concerning the phase separation issues for Mn and

(26) Zhou, F.; Kang, K.; Maxisch, T.; Ceder, G.; Morgan, D. *Solid State Commun.* **2004**, *132*, 181.
(27) Maxisch, T.; Zhou, F.; Ceder, G. *Phys. Rev. B* **2006**, *73*, 104301.
(28) Pantelides, S. T. *Phys. Rev. Lett.* **1986**, *57*, 2979.

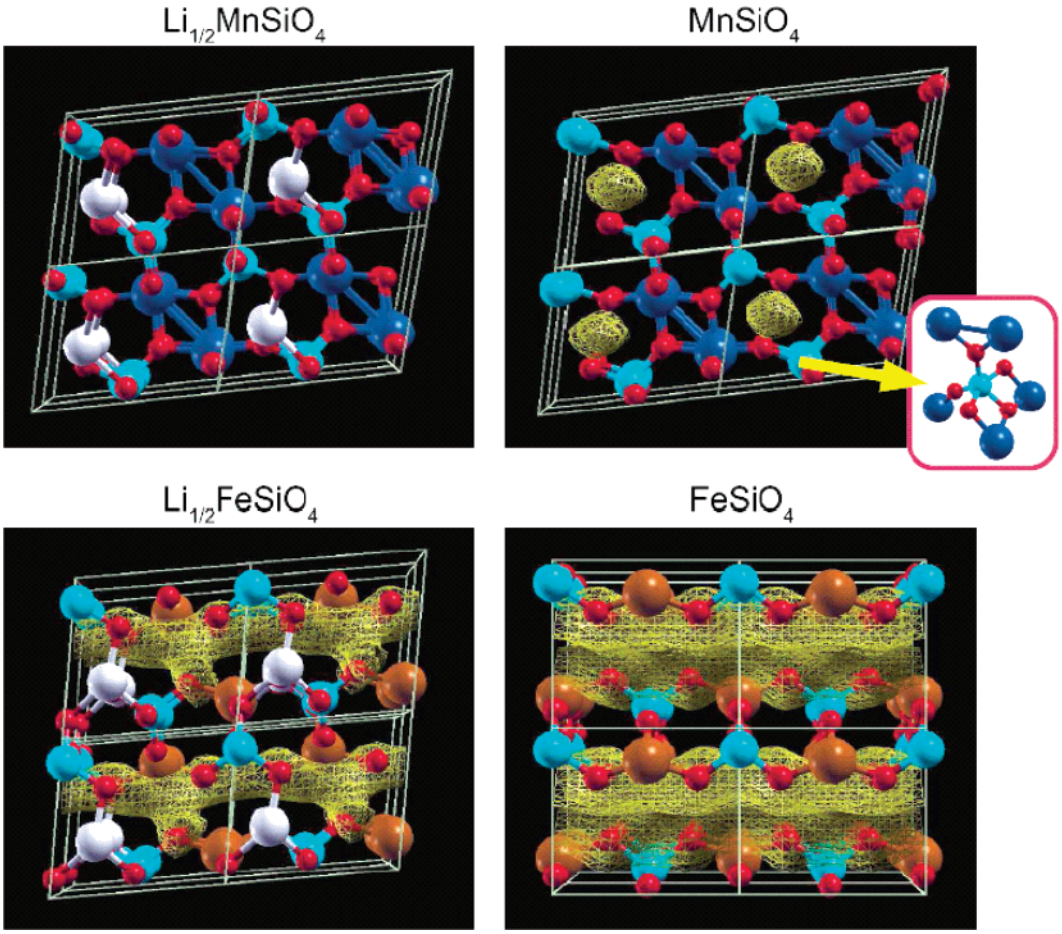

Figure 6. Snapshots of delithiated $Li_{0.5}MSiO_4$ and $MSiO_4$ structures, M = Mn (top) and Fe (bottom). Yellow isosurfaces (wired-style) show vacant regions in the structure. The inset shows a 5-fold coordinated Si found in the collapsed $MnSiO_4$ structure. The noncollapsed Fe structures are very open, whereas the collapsed Mn structures are compact (no vacant regions for $Li_{0.5}MnSiO_4$). Notice that the unit cells of the $Li_{0.5}MSiO_4$ are not orthorhombic but monoclinic—much more so for the collapsed Mn structure. This monoclinic shape of the unit cell might be an artifact because of final size effects, because the Li-vacancy pattern is restricted to the $(1 \times 1 \times 1)$ unit cell. Indeed, for collapsed $Li_{0.5}MnSiO_4$, we have identified a more stable, orthorhombic $(1 \times 2 \times 1)$ superstructure. In this superstructure, the Li-vacancy pattern of $(1 \times 1 \times 1)$ unit cell is alternating: the remaining Li ion is located in the bottom-left corner in the first cell and in the top-right corner in the next cell.

$Mn_{0.5}Fe_{0.5}$ compounds to be qualitatively altered, the difference in the TS_T terms should be as large as the TS_T value reported above, and its sign such as to counteract the $\Delta\epsilon(y)$.

At variance with our current prediction, Arroyo-de Dompablo et al.[12] predicted, by means of the GGA+U method, a negative formation energy for the pure Mn compounds. In particular, their calculated formation energies are −0.16 and −0.83 eV for the 50% delithiated $LiMnSiO_4$ and $LiFeSiO_4$, respectively, whereas our values are +0.16 and −0.88 eV, respectively. It is known that GGA may sometimes predict qualitatively wrong formation energies.[29] The current discrepancy for the Mn compound, however, has a different origin. In particular, our formation energy is calculated with respect to the more stable collapsed phase of fully delithiated $MnSiO_4$, whereas such a phase has not been identified in the literature.[12] If we recalculate the formation energy with respect to the less stable noncollapsed $MnSiO_4$ phase, we obtain −0.19 eV. Our GGA results are therefore in good agreement with those obtained using the GGA+U method,[12] provided that the same structures are assumed.

In a similar way to eq 2, the formation energy of the Mn/Fe mixing in the $Li_2Mn_xFe_{1-x}SiO_4$ can be calculated as $\Delta\epsilon(x) = \epsilon(x) - [x\epsilon(\mathrm{Mn}) + (1-x)\epsilon(\mathrm{Fe})]$, where ϵ(Mn) and ϵ(Fe) are total energies per FU of the pure Li_2MnSiO_4 and Li_2FeSiO_4, respectively. At $x = 0.5$, the calculated formation energy is only +4 meV/FU, a value smaller than our computational accuracy. According to this prediction, the $Mn_{0.5}Fe_{0.5}$ mixture should not phase separate at room temperature into Li_2MnSiO_4 and Li_2FeSiO_4 because of configurational entropy (ideal configurational entropy is 0.69 k_B/FU, the corresponding contribution to free energy at room-temperature would be $TS = 0.02$ eV/FU). However, other contributions to entropy (e.g., vibrational) may alter this conclusion.

4. Conclusions

In summary, the calculations predict, for the first time, that the structure of Li_2MnSiO_4 will collapse upon removal of large amounts of Li. The structural collapse has been experimentally undoubtedly confirmed using XRD, solid-state NMR and TEM investigations. These methods also reveal that the resulting structure is "amorphous-like". Moreover, as discussed above, during delithiation of Li_2MnSiO_4, a phase separation into Li_2MnSiO_4 and $MnSiO_4$ may occur. As the latter is amorphous-like, the amorphization can be observed already upon removal of smaller amounts

(29) Zhou, F.; Marianetti, C. A.; Cococcioni, M.; Morgan, D.; Ceder, G. *Phys. Rev. B* **2004**, *69*, 201101.

of Li, which can explain the drop in the reversible capacity during cycling. On the other hand, we have shown that, despite the loss of crystallinity, the resulting amorphous-like phase is still able to reversibly exchange a considerable amount of lithium. If the actual collapsed structure bares some local resemblance to the calculated $MnSiO_4$ structure (see Figure 6), we may speculate that Li ions can be accommodated within the egglike regions shown by the yellow isosurface. This would suggest that approximately 0.5 Li ions/FU can be exchanged. The measurements show a slightly higher reversible exchange, that is, about 0.7 Li/FU (see Figure 1b).

Unlike in the case of pure Li_2MnSiO_4, the calculations predict that the Mn/Fe mixture will not phase-separate during delithiation. Moreover, the potential required to extract more than 1 Li ion/FU is predicted to be substantially lower, by 0.7 V for $Li_xMn_{0.5}Fe_{0.5}SiO_4$, than that for the Fe compound, thus being within the present experimental reach (in the voltage range of up to 4.5 V). If the potential is controlled such that less than ~1.5 Li/FU is exchanged during the electrochemical cycling, the structure of the Mn/Fe mixture should not collapse. Thus, using an appropriate Mn/Fe mixture, it might be possible to obtain a stable material with a reversible exchange of more than one Li/FU. In spite of the fact that simulations allow for a stable Mn/Fe mixture, we have not been able to synthesize such a mixture so far. Using the known preparation routes, we have obtained either segregated phases of Li_2MnSiO_4 and Li_2FeSiO_4 (even if on the submicrometer scale) or phases with too large amounts of impurities to carry out a quantitative characterization. Thus, finding a route for preparation of homogeneous Mn/Fe mixtures with a high and stable capacity remains an exciting challenge for the future.

Acknowledgment. We thank Marie-Liesse Doublet for very useful discussions and Maja Remskar for performing TEM measurements. This work has been partially supported by the Slovenian Research Agency (Grant P2-0148).

Supporting Information Available: Discussion about the difference between the Mn- and Fe-compounds in terms of electronic structure, differential scanning calorimetry of Li_2MnSiO_4, measurement of specific heat, and GGA calculated density of states (PDF). This material is available free of charge via the Internet at http://pubs.acs.org.

CM063011L